Journal of
Nanoscience and Nanotechnology
Vol. 7, 3502–3508, 2007

The Influence of the Reaction Temperature on the Morphology of Sodium Titanate 1D Nanostructures and Their Thermal Stability

Polona Umek[1,*], Romana Cerc Korošec[2], Boštjan Jančar[1], Robert Dominko[3], and Denis Arčon[1,4]

[1] *Institute Jožef Stefan, Jamova 39, SI-1000 Ljubljana, Slovenia*
[2] *Faculty for Chemistry and Chemical Technology, Aškerčeva 5, SI-1000 Ljubljana, Slovenia*
[3] *National Institute of Chemistry, P.O.B. 660, SI-1001 Ljubljana, Slovenia*
[4] *Faculty for Mathematics and Physics, Jadranska 19, SI-1000 Ljubljana, Slovenia*

We have synthesized large quantities of sodium-titanate-based nanotubes and nanoribbons with high yields under hydrothermal conditions from anatase powder in an aqueous NaOH solution. The reaction temperatures were from 95 to 195 °C, in steps of 20 °C. We observed that the morphology of the nanomaterials, which is reflected in their specific surface areas, depends strongly on the reaction temperature. For the materials synthesized in the range 95–135 °C and above 155 °C only a single morphology type was observed for the nanostructures, i.e., nanotubes and nanoribbons, respectively. In contrast, when the reaction was carried out at 155 °C, both nanotubes and nanoribbons were found in the product. SEM, TEM, and XRD techniques were used to determine the materials' morphological and structural properties, and the thermal stability of the materials was investigated with TGA and DSC. The largest weight loss, of approximately 25%, was observed in a temperature range from 25 up to 600 °C for the product obtained at 95 °C, probably due to the presence of unrolled titanate sheets.

Keywords: Titanate Nanoribbons, Titanate Nanotubes, Hydrothermal Synthesis, TG/DSC.

1. INTRODUCTION

One-dimensional (1D) alkali titanates are one of the groups of inorganic materials being intensively studied in nanotechnology research. The family of alkali titanates represented by the general formula $A_2Ti_{2n}O_{2n+1}$ (A = Na, K, or Cs, and $3 \leq n \leq 6$) forms a variety of layered and channel-like structures. In the layered structures the alkali cations (A) occupy the interlayer space, while in the channel-like structures the cations are found along the channels. These kinds of structures enable good mobility of the alkali cations,[1] which is a necessary condition for the ion-exchange process to take place. For this reason the family of 1D titanates represents an attractive starting point for the design of different 1D titanates with a variety of morphologies and compositions.[2–4] 1D TiO_2 nanowires can also be produced by using the ion-exchange process followed by heat treatment.[5,6]

Alkali titanates are being intensively studied in bulk form for possible technological applications in the ion-exchange process, photocatalysis, as fuel-cell electrolytes, as reinforcement agents for plastics, and as gas sensors.[7–11] Furthermore, for the case of 1D titanate nanomaterials, it is expected that their physical and chemical properties will be enhanced in comparison to the titanates in bulk form. It is thought, for example, that pristine sodium titanate nanotubes (NTs) and the 1D nanomaterials derived from them could be promising materials for energy storage based on lithium insertion.[3,5,12–14] In the field of catalysis, titanate NTs can be exploited as a catalyst support because of their large specific surface area.[15] On the other hand sodium titanate nanoribbons (NRs) exhibits the catalytic ability for reduction of $NO_{2(g)}$ to $NO_{(g)}$ (Ref. [16]). It is likely that sodium titanate NRs could also be used for the reinforcement of a polymer matrix, since their Young's moduli[17] are comparable to that of carbon nanotubes grown by CVD.[18]

1D sodium titanates are obtained at low temperatures under hydrothermal conditions from TiO_2 in an alkali solution. After the first publications of Kasuga et al. on the synthesis of sodium titanate NTs[19,20] the hydrothermal method has become one of the most popular techniques for the preparation of 1D titanate nanomaterials. In addition,

*Author to whom correspondence should be addressed.

1533-4880/2007/7/3502/007 doi:10.1166/jnn.2007.838

a change of reaction conditions can result in the direct formation of nanowires (NWs)[21–23] and NRs[3, 16, 24] as well as titanate NTs.[15, 25–27]

Up to now there have been reports on the preparation of titanate NTs and NRs based on a range of TiO_2 precursors: amorphous,[22, 24] anatase,[2, 28–30] rutil,[26, 31] brookite,[23] or a mixture of anatase and rutil.[15, 28] Whether it is titanate NTs, NWs or NRs that are formed depends to a large extent on the reaction temperature; however, there is no doubt that other reaction conditions, like the form of the TiO_2 precursor and the concentration of the NaOH, also have an influence on the morphology and dimensions of the resulting 1D titanate nanostructures. This becomes clear when one compares the dimensions of the NTs synthesized from different TiO_2 precursors (rutil, anatase, amorphous TiO_2, or metallic titanium).[15, 16, 25, 28] The dimensions of the resulting NTs are thus strongly reflected in the values of the specific surface area. The specific surface areas of NTs obtained from different TiO_2 precursors are in the range 100–450 m^2/g. The highest values reported for the specific surface area of titanate NTs were obtained when using TiO_2 powder in the rutil form[26] or where the TiO_2 powder was a mixture of anatase and rutil.[15, 32]

However, to the best of our knowledge the temperature dependence of the formation of the NT and NR morphologies beginning with an anatase TiO_2 precursor has not yet been discussed. In this work we investigated the influence of the reaction conditions on the morphology of the resulting sodium titanate NTs and NRs. Under the applied conditions both NTs and NRs were synthesized in large quantities, with yields above 90% (as estimated from the SEM and TEM images). We also show that the specific surface area can be regulated by the reaction temperature and by smaller extent with the average particle size of the anatase. In this paper we also discuss the thermal stability of the products obtained under hydrothermal conditions between 95 and 195 °C.

2. EXPERIMENTAL DETAILS

2.1. Synthesis of Sodium Titanate Nanotubes and Nanoribbons, and Adsorption

Sodium titanate nanotubes and nanoribbons were synthesized using a similar procedure to that reported by Kasuga et al.,[20] i.e., 4.40 g of fine anatase TiO_2 powder (Aldrich, 9 m^2/g (average particle size ~1 μm) and 200 m^2/g (average particle size ~20 nm) was dispersed in 30 ml of 10 M NaOH (Aldrich) with the help of an ultrasonic bath. Then 30 ml of the reaction mixture was transferred into a 33-ml Teflon-lined autoclave (the degree of filling was 90.9%) and held at different temperatures (95, 115, 135, 155, 175, and 195 °C) for 72 hours. The resulting white powders were first dispersed in 200 ml of deionized water and filtered. The material caught on the filter was subsequently washed with 50 ml of ethanol. Finally, the isolated product was dried overnight at 70 °C. A typical reaction batch produced around 6.5 g of material. Materials for the XRD and BET analysis were dried overnight at 150 °C before the measurements.

2.2. Instrumentation

The morphology of the synthesized materials was investigated with scanning (SEM, Supra 35 LV) and transmission (TEM, Jeol-JEM 2000F and Jeol JEM-2010, both 200 keV) electron microscopes. The materials for the TEM observations were dispersed by sonication in methanol, with the drop of dispersion deposited on a copper TEM grid covered with a carbon foil. The samples for the SEM observations were simply pressed onto a conducting carbon tape.

The BET specific surface areas of the samples were measured at −196°C with a TRISTAR 3000 automated gas-adsorption analyzer.

The powder X-ray diffraction (XRD) patterns were obtained on a Bruker AXS D4 Endeavor diffractometer using Cu K_α radiation.

The dynamic thermogravimetric (TG) measurements were performed on a Mettler Toledo TGA/SDTA 851^e from room temperature up to 600 °C, with a heating rate of 5 K/min. Approximately 1 mg of the sample was placed in a 20-μl aluminum crucible and then covered with a pierced lid. Nitrogen, with a flow rate of 100 ml/min, was used as a purge gas. The baseline was subtracted in all cases.

The DSC analysis was carried out on a Mettler Toledo DSC 822^e Cell. The experimental conditions (sample pan, size of the sample, heating rate, atmosphere, and flow rate) were the same as used for the TG measurements. An empty pan served as the reference.

3. RESULTS AND DISCUSSION

The morphological evolution for the reaction temperatures between 195 and 135 °C for the hydrothermally treated micrometer-sized anatase particles is presented in Figure 1. The SEM images of the products obtained at 195 °C (**195-NRs**, Fig. 1(a)) and 135 °C (**135-NTs**, Fig. 1(c)) demonstrate that the morphologies of the samples are very different. In the sample synthesized at 155 °C (**155-NR + NTs**), i.e., at the medium reaction temperature, both types of morphologies are observed (Fig. 1(b)). Further investigations using a TEM showed that the structures obtained at 165 °C and higher have a nanoribbon-like morphology (Fig. 2(a)), while the structures obtained below 155 °C are nanotubes (Fig. 2(b)). Regardless of the reaction temperature the nanoribbons exhibit a broad size distribution. Their lengths are between 500 nm and several micrometers, with typical widths varying from 30 to 300 nm.

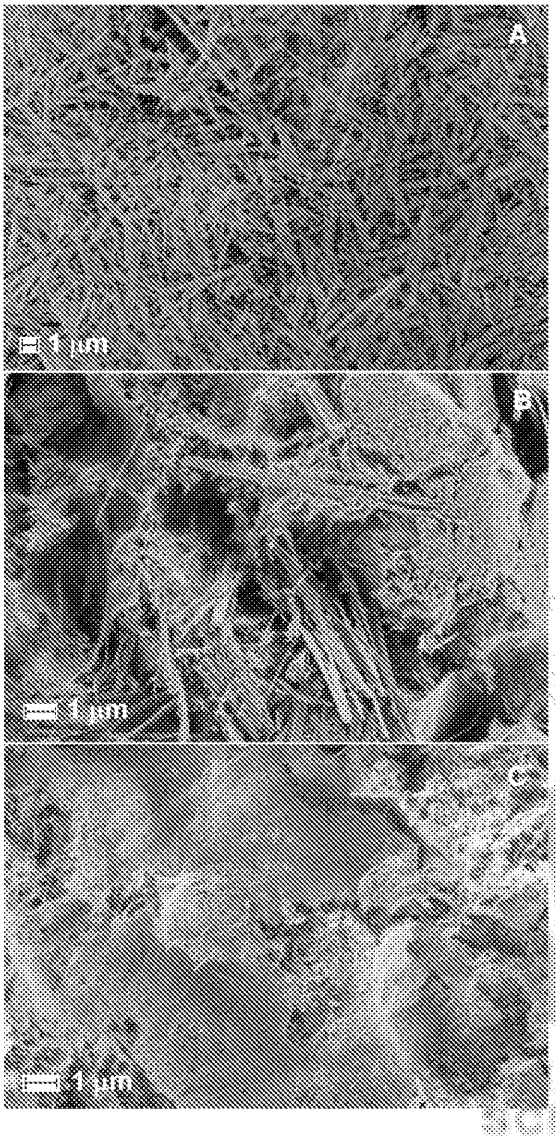

Fig. 1. SEM images of 1D titanate materials synthesized at 195 (A), 155 (B), and 135 °C (C). At 155 °C, the medium reaction temperature, structures with two different morphologies are formed.

The heights of these structures were measured by AFM, and range from 15 to 60 nm.[17] Comparing the lengths of both types of nanostructures shows that the NTs are much shorter, as they only achieve lengths up to 500 nm. The average outer diameter of the observed NTs (TEM observations) synthesized at 115 (Fig. 2(b)) and 135 °C is 10 nm, with the inner diameter ranging between 3 and 5 nm.

The product synthesized at the lowest investigated reaction temperature, i.e., 95 °C, (**95-NTs,** Fig. 2(c)) is mainly composed of NTs. Under the TEM a considerable number of partly rolled titanate sheets were observed (the arrows in Fig. 2(c) point to these sheets). The presence of these unrolled titanate nanosheets supports the proposed formation mechanism of the titanate nanotubes.[33–35] This is also supported by the fact that titanate NTs can be formed from layered $Na_2Ti_3O_7$ (Ref. [27]). Under the applied reaction conditions the dominant morphology in the obtained product was found to be incompletely rolled titanate sheets.

The influence of anatase particles with an average diameter of 20 nm on the dimensions of the formed titanate NTs was also investigated. In this case, the produced NTs form aggregates resembling see-urchin-like structures. This secondary structure of the material obtained at 115 °C from a nanosized TiO_2 precursor (**115n-NTs**) is presented in Figure 3. The so-formed aggregates cannot be dispersed into individual NTs, even after prolonged sonication, and therefore we could not estimate the actual lengths of the NTs. Using a hydrothermal treatment of titanium metal Mao et al.[15] also observed see-urchin-like aggregates, formed from NTs of approximately the same size and shape.

The literature contains much debate about the exact structure of sodium-titanate-based nanotubes and nanoribbons. For the nanotubes two similar structures are proposed: $(Na,H)_2Ti_3O_7$ [2, 32, 34] and $(Na,H)_2Ti_2O_4(OH)_2$.[28, 36, 37] ESEEM (electron spin-echo envelope modulation) measurements on the local structure favor the second of these structures.[16] In the case of nanoribbons, various authors[4, 22, 32] propose the same, i.e., the $(Na,H)_2Ti_3O_7$ structure, which agrees well with the XRD spectra.

The evolution of the XRD spectra with respect to reaction temperature (Fig. 4) is in agreement with our morphology studies. The products containing NTs, (**95, 115, 135-NTs**) and also **155-NTs + NRs**, where nanotubes are the dominant morphology, reveal a single type of XRD spectra. A second type of spectra, in which sharp peaks appear, is typical for the NR samples (**175** and **195-NRs**). The characteristic spectra of the NT samples synthesized between 95 and 135 °C contain broad diffraction peaks with intensities that progressively increase with increasing reaction temperature. This broadening of the diffraction peaks can be attributed to the nanometer dimensions of the tubes and also to their poor crystallinity. Using the Scherrer formula ($d = 0.9\lambda/B\cos\theta$, where λ is the wavelength, B is the width at the half height of the Bragg peak, and θ is the Bragg angle) we estimated the average diameter (from the 110 peak[29] positioned at approximately 24.3 degrees, Fig. 4) to be in the range from 7 to 15 nm. The obtained values correspond to the outer diameter of the obtained nanotubes. In contrast, sharp peaks are observed in the spectra of the NR samples, as a result of the increased crystallinity.[16] We also calculated the values for the average particle size of the NR samples (from the 110 peak,[38] Fig. 4) using the Scherrer formula. The obtained number—from 25 (**175-NRs**) to 35 nm (**195-NRs**)—corresponds well with the measured heights of the NRs.

The closest match to the XRD spectra collected from the samples synthesized above 155 °C appears to be a spectrum of layered $Na_2Ti_3O_7$ (JCPD 72-0148). However, there is a mismatch between some of the peak positions, and some additional peaks are present in the collected spectra. These observations imply that the crystal structure of

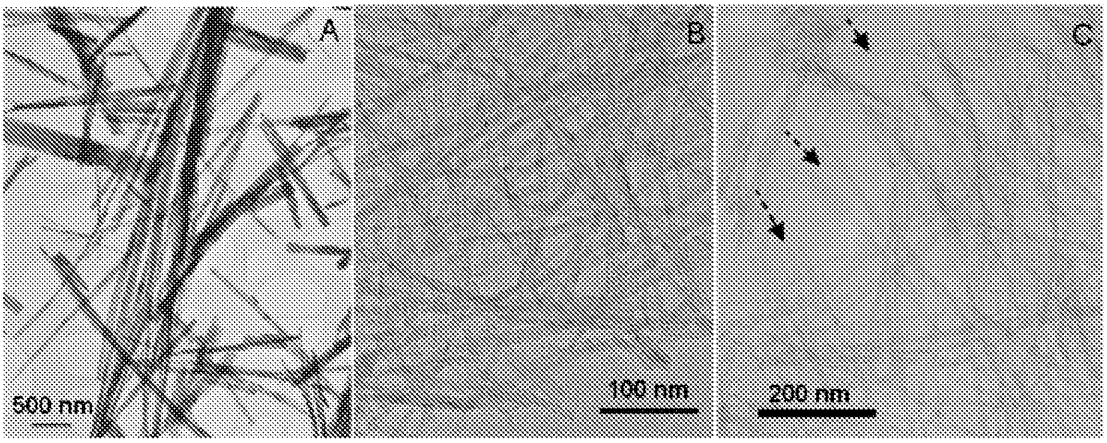

Fig. 2. TEM images of samples synthesized at 165 (A), 115 (B), and 95 °C (C). The arrows in 2(C) point to unrolled titanate sheets.

the hydrothermally synthesized nanoribbons deviates from the structure of $Na_2Ti_3O_7$, which is characterized by corrugated ribbons of three edge-sharing TiO_6 octahedra joined via corners and interleaved with Na^+ ions.[1] This deviation could be the result of some degree of exchanging of these interlayer alkali-metal ions, to which such structures are prone.[1]

Additional information can be obtained from the typical electron diffraction (ED) pattern, shown in Figure 5, collected from a single nanoribbon. The extinguished reflections suggest that the monoclinic unit cell of the nanoribbon is C-centered rather than primitive, which is characteristic of $Na_2Ti_3O_7$. Furthermore, the ED pattern reveals that the longer dimension of the nanoribbons extends in the direction parallel to the [010] axis of the layered structure. As is common to all of the monoclinic layered sodium titanates, the [010] direction runs parallel to the interlayer occupied by the alkali metal ions.

The difference in the morphologies of the obtained NTs and NRs is reflected in their specific surface area. As would be expected, the values for the active surface area are very different for the NR and NT structures. The active surface areas of the NTs synthesized at 95, 115, and 135 °C range from 190 to 240 m^2/g, while for the nanoribbon materials the surface areas are below 30 m^2/g. The influence of the precursor particles' size on the specific surface areas of the NTs was also investigated. Two different anatase powders were used for the syntheses: the first synthesis used micrometer-sized powders, and the second used nanometer-sized particles. We observed that the precursor with the smaller size particle gave only a slightly

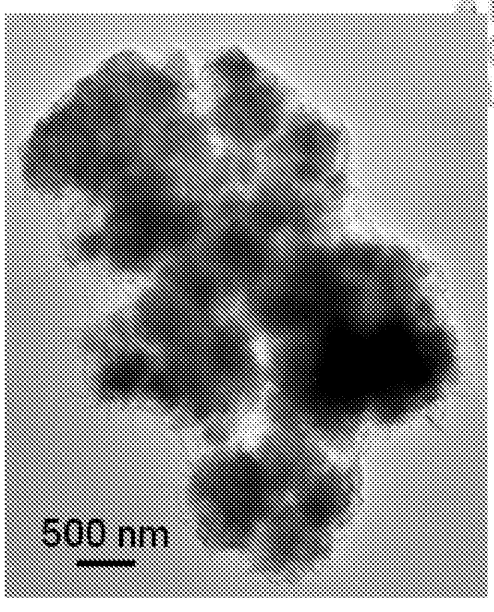

Fig. 3. Typical TEM image of titanate NTs synthesized at 115°C, beginning with 20-nm-sized anatase particles (**115n-NTs**). Aggregates resembling a see-urchin-like structure are clearly observed.

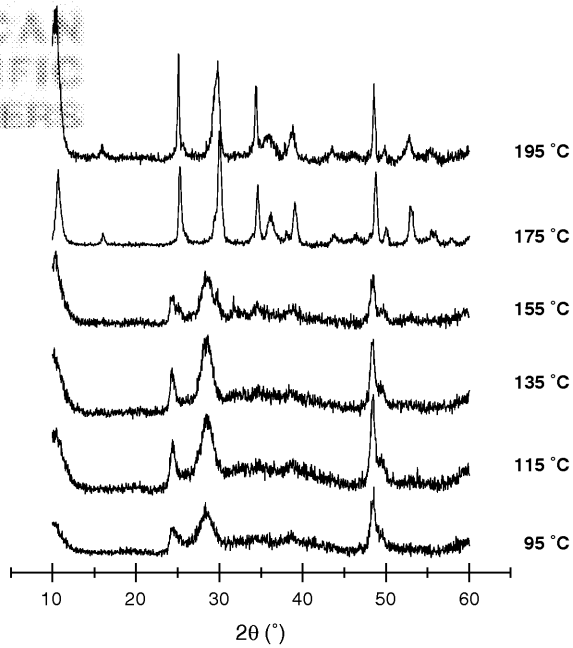

Fig. 4. Powder XRD patterns of materials synthesized between 95 and 195 °C.

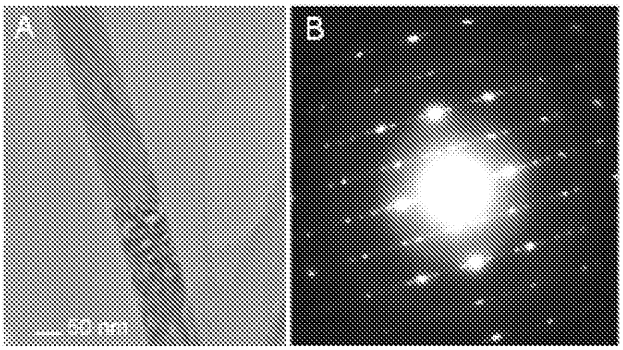

Fig. 5. TEM image of an individual nanoribbon synthesized at 175 °C (A) with the corresponding electron diffraction pattern (z = [001]) (B).

increased specific surface area. For instance, if we compare the NTs synthesized at 115 °C (the sample with the largest specific surface area) from micrometer (**115-NTs**) and nanometer (**115n-NTs**) sized anatase particles is the increase in BET surface area relatively small (from 240 (**115-NTs**) to 250 m^2/g (**115n-NTs**)).

Figure 6 shows typical isotherms for N_2 adsorption onto the nanotubes and nanoribbons synthesized at 115 and 195 °C. A comparison of the **115-NT** and **195-NR** isotherms clearly indicates that the **115-NT** product is predominantly mesoporous. The pore-size distribution of the samples synthesized at 115 and 135 °C, calculated from the adsorption data, is shown in Figure 7. The maxima for the **115** and **135-NTs** are observed in two regions. In the first region, two peaks appear at 2.1 nm and 3.4 nm, respectively. These two peaks are considered to correspond to the inner diameter of the NTs, which is in relatively good agreement with the TEM observations. It is likely that the smaller diameter calculated from the pore-size distribution when compared to the values obtained with the TEM is the result of dangling bonds inside the nanotubes (which are in fact nanorolls) that cling to the inner walls[39] and thus decrease the volume of the NTs. The origin of

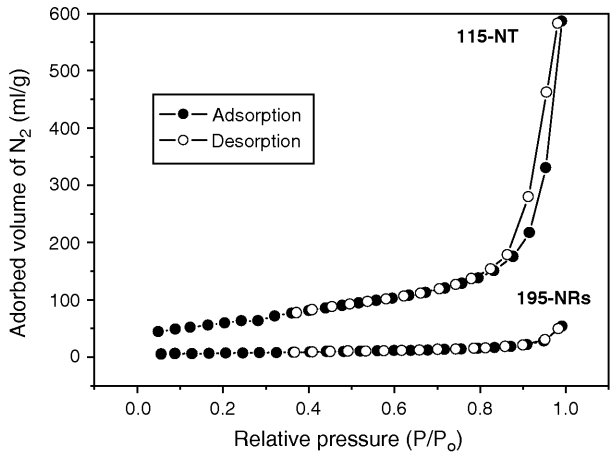

Fig. 6. N_2 adsorption isotherms at −196 °C for titanate nanoribbons and nanotubes synthesized at 195 °C and 115 °C, respectively.

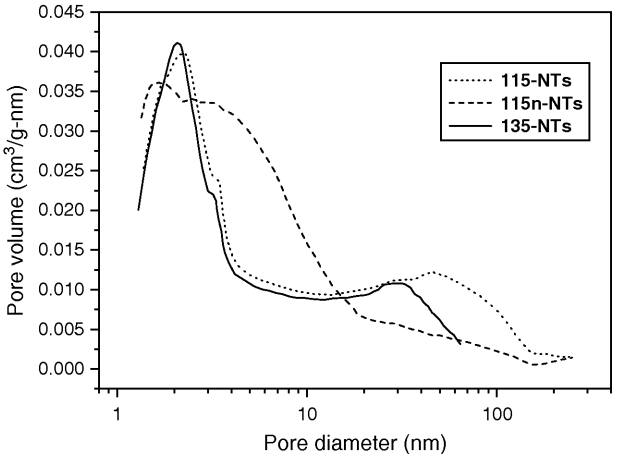

Fig. 7. Pore-size distribution of samples synthesized at 115 and 135°C. **115n-NTs** were synthesized from nanometer-sized anatase TiO_2 powder, while for the synthesis of **115-NTs** and **135-NTs** micro-sized anatase TiO_2 powder was used.

the second peak between 25 and 70 nm is more difficult to explain. First, in these two samples no nanotubes with diameters exceeding 17 nm were observed; so most probably this broad peak is caused by the aggregation of NTs.[20] For the **115n-NTs** sample maxima were only observed in the first region at 1.7 and 3.0 nm. From a comparison of the pore-size-distribution curves for the **115**, **115n**, and **135-NTs** samples it can be concluded that the reaction temperature has a relatively small effect on the inner diameters of the formed NTs. A slightly larger effect on the distribution of the inner diameters results from smaller-sized anatase particles.

We now turn to the thermal stability of the obtained products. Thermogravimetric curves of materials, synthesized at 95, 135, 155, and 195 °C, measured in a temperature range from 25 up to 600 °C, are shown in Figure 8(a). In general, the greater part of the weight loss occurs at lower temperatures, where the dehydration of physisorbed water takes place. On a DSC curves (Fig. 8(b)) this process is reflected in two successive endothermic peaks. From both Figures (8(a) and 8(b)) it is evident that there is a lower content of the physisorbed water in materials, synthesized at higher temperatures. Water molecules are also more tightly bonded than in materials, synthesized at lower temperatures (see dashed line in Fig 8(a)). For **95-NTs** the weight loss of approximately 17% occurs up to 150 °C, while the sample **195-NRs** loses only 8.5% up to 200 °C. After this temperature the weight slowly and continuously decreases nearly up to 600 °C. It was already found out that for nanotubed $H_2Ti_2O_4(OH)_2$ at temperatures lower than 300 °C desorption of physically adsorbed water and interlayered water takes place simultaneously.[28] At higher temperatures (300–500 °C) desorption of interlayered water leads to transition from orthorobmic crystal system to anatase. The last process is reflected as an exothermic peak on a DSC curve.[28] For our materials,

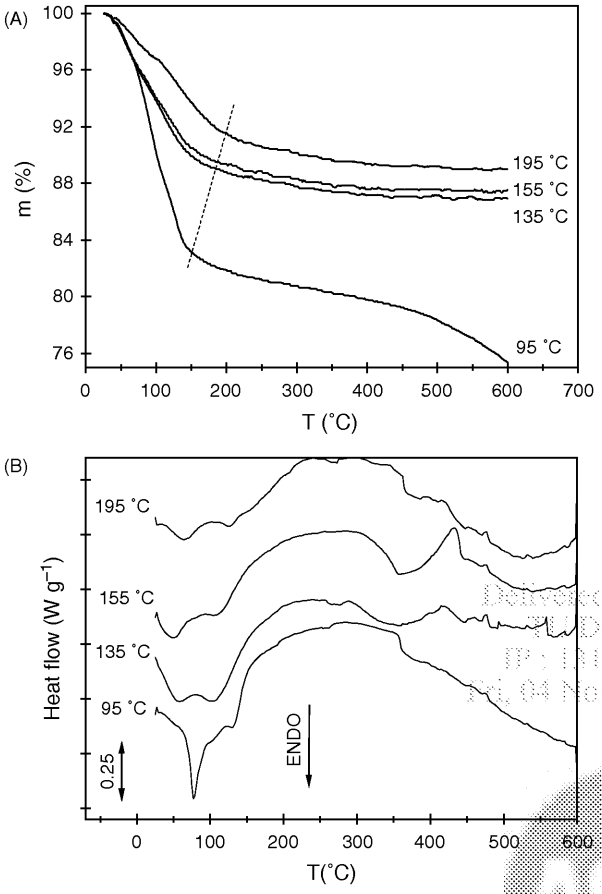

Fig. 8. Comparison of TGA (A) and DSC (B) curves for sodium titanate nanotube and nanoribbon samples measured between room temperature and 600 °C. The curves correspond to materials synthesized at 95, 135, 155, and 195 °C.

the dehydroxilation of intralayered OH groups is separated from the dehydration of physically adsorbed water and occurs in a temperature range from 200 °C up to 400 °C. Exothermic process, accompanying the formation of new Ti–O–Ti bonds, overwhelms endothermic dehydration process and is reflected as a broad exothermic peak on the DSC curves.

Dehydroxilation of interlayered OH groups occurs at temperatures higher than 400 °C and is observed only for **135-NTs** and **155 NTs + NRs**. Sample **95-NTs** behaves differently probably due to the presence of unrolled titanate sheets. Besides that it contains the biggest amount of physisorbed water, its weight start to decrease more rapidly at temperatures higher than 400 °C, meaning that the material is thermally unstable. The total weigh loss of almost 25% between room temperature and 600 °C was observed for this sample, while for material synthesized at 135 and 155 °C very similar weight loss of around 13% was detected. The latter fact is suggesting that the dominant morphology in **155-NTs + NRs** are nanotubes. This is in agreement with SEM image of **155-NTs + NRs** (Fig. 1(b)), specific surface area and XRD spectrum (Fig. 3). The smallest weight loss of 11% was observed for **195-NRs.** The measured value was expected due to different morphology (hollow structure of NTs versus full layered structure of NRs) and agrees with EPR (electron paramagnetic resonance) measurements.[16] Broad exothermic peak in a temperature range from 200 to 500 °C on the DSC curve means that material, synthesized at 195 °C, loose intralayered OH groups in a broader range while interlayered OH groups remain in the structure up to 600 °C or the cleavage of both type of OH groups occurs simultaneously. Additional XRD measurements should be done in order to elucidate this process.

4. CONCLUSIONS

Both titanate $(Na,H)_2Ti_2O_4(OH)_2$ nanotubes and $(Na,H)_2Ti_3O_7$ nanoribbons were synthesized in gram quantities. The nanotubes were formed in the temperature range from 115 and 135 °C, while the nanoribbons were obtained at temperatures higher then 155 °C. The product yield was very high for all the reaction temperatures, except for 155 °C, where both morphologies formed under the applied conditions. This study also revealed that the reaction temperature has a more pronounced effect on the specific surface area of the resulting nanotubes than a smaller size of anatase particles.

Acknowledgments: The financial support from the Ministry of Higher Education, Science and Sport of the Republic of Slovenia and the Gorenje d.d.–Innovation Centre, an industrial partner, is greatly acknowledged. The authors would like to thank to U. Pirnat, B.Sc., for making the XRD measurements.

References and Notes

1. T. P. Feist and P. K Davies, *J. Solid State Chem.* 101, 275 (**1992**).
2. R. Yoshida, Y. Suzuki, and S. Yoshikawa, *Mat. Chem. Phys.* 91, 409 (**2005**).
3. R. Dominko, E. Baudrin, P. Umek, D. Arčon, M. Gaberšček, and J. Jamnik, *Electrochem. Commun.* 8, 673 (**2006**).
4. Y. V. Kolen'ko, K. A. Kovnir, A. I. Gavrilov, A. V. Garashev, J. Frantt, O. I. Lebedev, B. R. Churugulov, G. van Tendeloo, and M. Yoshimura, *J. Phys. Chem. B* 110, 4030 (**2006**).
5. A. R. Armstrong, G. Armstrong, J. Canales, and P. G. Bruce, *Angew. Chem. Int. Ed.* 43, 2286 (**2004**).
6. R. Yoshida, Y. Suzuki, and S. Yoshikawa, *J. Solid State Chem.* 178, 2179 (**2005**).
7. I. M. El-Naggar, E. A. Mowofay, I. M. Ali, and H. F. Aly, *Adsorption* 8, 297 (**2002**).
8. J. H. Choy, H. C. Lee, H. Jung, and S. J. Huang, *J. Mater. Chem.* 11, 2232 (**2001**).
9. D. J. D. Corcoran, D. P. Tunstall, and J. T. S. Irvin, *Solid State Ionics* 136, 297 (**2000**).
10. J. Lu and X. Lu, *J. Appl. Polym. Sci.* 82, 368 (**2001**).
11. M. W. Anderson and J. Klinowski, *Inorg. Chem.* 29, 3260 (**1990**).
12. Y. Zhou, L. Cao, F. Zhang, B. He, and H. Li, *J. Electrochem. Soc.* 120, A1246 (**2003**).

13. L. Kavan, M. Kalbč, M. Zukalova, I. Exnar, V. Lorenzen, R. Nesper, and M. Graetzel, *Chem. Mat.* 16, 477 (**2004**).
14. J. Li, Z. Tang, and Z. Zhang, *Chem. Mat.* 17, 5848 (**2005**).
15. C.-C. Tsai and H. Teng, *Chem. Mat.* 16, 4352 (**2004**).
16. P. Umek, P. Cevc, A. Jesih, A. Gloter, C. P. Ewels, and D. Arčon, *Chem. Mat.* 17, 5945 (**2005**).
17. M. Humar, D. Arčon, P. Umek, M. Škarabot, I. Muševič, and G. Bregar, *Nanotechnology* (**2006**), submitted.
18. B. Lukić, J. W. Seo, R. R. Basca, S. Delpeux, F. Beguin, G. Bister, A. Fonseca, J. B. Nagy, A. Kis, A. J. Kulik, and L. Forro, *Nanoletters* 5, 2074 (**2005**).
19. T. Kasuga, M. Hiramatsu, A. Hoson, and T. Sekino, *Langmuir* 14, 3160 (**1998**).
20. T. Kasuga, M. Hiramatsu, A. Hoson, and T. Sekino, *Adv. Mat.* 11, 1307 (**1999**).
21. Z.-Y. Yuan and B.-L. Su, *Colloids and Surfaces A Physicochem. Eng. Aspects* 241, 173 (**2004**).
22. D. Wu, J. Li, X. Zhao, A. Li, Y. Chen, and N. Ming, *Chem. Mat.* 18, 547 (**2006**).
23. X.-D. Meng, D.-Z. Wang, J.-H. Liu, and S.-Y. Zhang, *Mat. Res. Bull.* 39, 2163 (**2004**).
24. Z. Y. Yuan, J.-F. Colomer, and B.-L. Su, *Chem. Phys. Lett.* 363, 362 (**2002**).
25. Y. Mao, M. Kanungo, T. Hemraj-Beny, and S. S. Wong, *J. Phys. Chem. B* 110, 702 (**2006**).
26. A. Thorne, A. Kruth, D. Tunstall, J. T. S. Irvine, and W. Zhou, *J. Phys. Chem. B* 109, 5439 (**2005**).
27. M. Wei, Y. Konishi, H. Zhou, H. Sugihara, and H. Arakawa, *Solid State Commun.* 133, 493 (**2005**).
28. M. Zhang, Z. Jin, J. Zhang, X. Guo, J. Yang, W. Li, X. Wang, and Z. Zhang, *J. Mol. Catalysis A Chemical* 217, 203 (**2004**).
29. D. Wu, J. Liu, X. Zhao, A. Li, Y. Chen, and N. Ming, *Chem. Mat.* 18, 547 (**2006**).
30. Q. Zhao, Gao, J. Sun, and S. Zheng, *Chem. Lett.* 1202 (**2002**).
31. Y. Suzuki and S. Yokishava, *J. Mat. Res.* 19, 982 (**2004**).
32. C.-C. Tsai and H. Teng, *Chem. Mat.* 18, 367 (**2006**).
33. S. Zhang, L.-M. Peng, Q. Cheng, G. H. Du, G. Dawson, and W. Z. Zhou, *Phys. Rev. Lett.* 91, 256103-1 (**2003**).
34. Y. Q. Wang, G. Q. Hu, X. F. Duan, H. L. Sun, and Q. K. Xue, *Chem. Phys. Lett.* 365, 427 (**2002**).
35. B. D. Yao, Y. F. Chan, X. Y. Zhang, W. F. Zhang, and N. Wang, *Appl. Phys. Lett.* 82, 281 (**2003**).
36. C. Zhang, X. Jiang, B. Tian, X. Wang, X. Zhang, and Z. Du, *Colloids and Surfaces A Physicochem. Eng. Aspects* 257, 173 (**2005**).
37. J. Yang, Z. Jin, X. Wang, W. Li, J. Zhang, S. Zhang, X. Guo, and Z. Zhang, *Dalton. Trans.* 3898 (**2003**).
38. J. Yang, D. Li, X. Wang, X. Yang and L. Lu, *J. Mat. Science* 38, 2907 (**2003**).
39. A. E. Enyashin and G. Seifert, *Phys. Stat. Sol. B* 242, 1361 (**2005**).

Received: 15 May 2006. Revised/Accepted: 10 September 2006.